

THE MAXIMUM ENTROPY FORMULATION OF INVERSE PROBLEMS OF NDE

R.M. Bevenssee

Lawrence Livermore National Laboratory
Livermore, CA 94550

INTRODUCTION

This paper introduces the Maximum Entropy method of resolving underdetermined objects (flaws or inclusions) by a physicists' brand of nonlinear processing of the image data. We survey three areas of research: (1) synthetic aperture imaging to resolve three dimensional flaws, with the aid of selective back projection, (2) scattering from anomalies according to the inhomogeneous Fredholm integral equation of the second kind, and (3) ultrasonic flaw characterization by the boundary integral equation method. A simple example is offered to illustrate the potential resolving power of the ME method for problems in area (2). We present some criteria for effective ME inversion.

SYNTHETIC APERTURE RESOLUTION OF 3D FLAWS, WITH THE AID OF SELECTIVE BACK PROJECTION

Researchers at Stanford University have reported on the success of their 50 MHz imaging system to locate defects in ceramics.¹ They employ a square synthetic aperture to image flaws in flat samples and a cylindrical aperture to find flaws in rods. Their point-spread functions which describe the propagation of waves from object point to image point are accurately known.

The point spread function (PSF) from objective point (x, y, z) to image point (x_0, y_0, z_0) in the square aperture system is

$$T(x,y) \text{ at constant } z \approx \frac{\sin[\theta_D(x-x_0)] \sin[\theta_D(y-y_0)]}{\sin[\theta_\lambda(x-x_0)] \sin[\theta_\lambda(y-y_0)]} \quad (1)$$

where

$$\theta_D = \pi 2D/\lambda z \quad \theta_\ell = \pi 2\ell/\lambda z$$

D = aperture width, ℓ = element spacing

The aperture is undersampled by a factor of 4 (λ_c , the center frequency wavelength, is $\approx D$ rather than $D/4$). Undesirably high sidelobe levels therefore occur.

In the cylindrical aperture system the PSF is

$$T(z) \text{ at constant } R, \theta \approx \frac{\sin[\theta_z (z-z_0)]}{\sin[\theta_\ell (z-z_0)]} \tag{2}$$

where

$$\theta_z = \pi 2D_z/\lambda R \quad , \quad D_z = z\text{-width of aperture}$$

$$\theta_\ell = \pi 2\ell_z/ R \quad , \quad \ell_z = \text{element spacing in } z.$$

The backscatter from a defect falls within an image region of strong reinforcement and an outer region where the contributions tend to cancel.

To reduce sidelobe levels a limited angular aperture is employed to eliminate those rays from the object which are outside the region of discrimination. Although this method effectively reduces sidelobe levels, it does discard image information, contrary to the ME philosophy by which all relevant data are retained and a minimum of assumptions are made about unavailable data.

An ME method has been applied successfully to the analogous problem of photon image enhancement in a square aperture system.² Let $\hat{p}_i(\vec{r}_i)$ denote the probability of photons from the i^{th} object pixel at position \vec{r}_i and $t(\vec{r}_i, \vec{r}_k')$ be the transmission factor analogous to T of (1) from \vec{r}_i to image pixel \vec{r}_k' . If $B(\vec{r}_k')$ is the measured brightness the quantity

$$\sum_{i \text{ object}} [\hat{p}_i(\vec{r}_i) t_{ik}(\vec{r}_i, \vec{r}_k')]^2$$

is the squared deviation between predicted and measured brightness due to noise in the k' pixel and

$$E\{\hat{p}_i\} = \sum_{k, \text{ image}} \sum_{i, \text{ object}} [p_i t_{ik} - B_k]^2 \tag{3}$$

is the noise "energy" in the image. The ME method seeks the most probable distribution of the \hat{p}_i subject to energy E being a minimum or less than a known noise level.

The entropy H is the logarithm of the total number of distinct

combinations of photon intensities on the object and, by Stirling's formula, is proportional to

$$H = -\sum_i \hat{p}_i (\ln \hat{p}_i - 1) \tag{4}$$

In maximizing H relative to the \hat{p}_i subject to constraints it is convenient to utilize Lagrange's method of undetermined multipliers and maximize instead the "objective" function F

$$F = \beta E\{\hat{p}_i\} + H + \gamma (\sum \hat{p}_i - 1). \tag{5}$$

Here β is a weight factor for the noise selected a priori, and γ is the multiplier chosen to constrain the convenient normalization $\sum \hat{p}_i = 1$. The ME equations for the \hat{p}_i are obtained by setting $\partial F / \partial \hat{p}_i = 0$ for all i.

As an example of the ME resolution possible Fig. 1(a) shows² a flat object on a 20 x 20 grid of binary pixels and (b) is the diffraction limited image. The ME resolution becomes extremely sensitive to β when it becomes large; the resolution for $\beta = 10^7$ is shown in (c).

The foregoing ME reconstruction was carried out in real space; reconstruction in wavenumber space has been performed in radio astronomy, and radio stars have been well resolved with the conventional Fourier transform background noise largely suppressed.³

ELASTIC WAVE SCATTERING BY VOIDS AND INCLUSIONS

Gubernatis⁴ has presented the exact equations for three dimensional scattering of an incident shear or compressional wave by a volume anomaly. We shall now summarize a preliminary investigation of a simplified situation to see if the ME method shows any promise for resolving volume anomalies from scatter data.

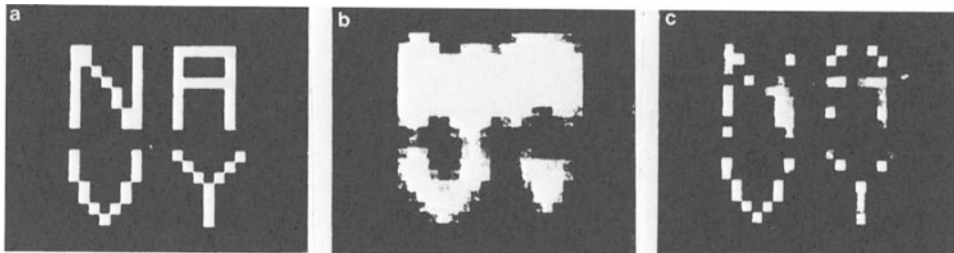


Fig. 1. ME resolution of a flat object from its diffraction limited image. (a) object defined on a 20x20 grid of binary pixels, (b) image, (c) resolution with $\beta = 10^7$.

For our assessment we assumed a compressional (or shear) wave characterized by one component, scattering from a two dimensional anomaly in an infinite medium with neither coupling between components nor wave mixing. The equation for the monochromatic total scalar displacement $u(\vec{r})$ is

$$u(\vec{r}) = u^0(\vec{r}) + \int d\vec{r}' g(\vec{r}, \vec{r}') v(\vec{r}') u(\vec{r}') \tag{6}$$

with u^0 the incident (plane) wave and Green's function g being

$$g(\vec{r}, \vec{r}') = \frac{k_o^2}{4\pi\rho\omega^2} \frac{e^{-ik_oR}}{R(\vec{r}, \vec{r}')} , \quad k_o = \frac{\omega}{v_p} = \frac{2\pi}{\lambda} \tag{7}$$

ρ = density, ω = circular frequency, v_p = phase velocity, λ = wavelength, and the time dependence is $\exp(i\omega t)$. $v(\vec{r}')$ describes the void or inclusion as

$$v(\vec{r}') = \delta\rho\omega^2\theta(\vec{r}') \tag{8}$$

where $\delta\rho$ = change in ρ from the infinite-medium value, and $\theta(\vec{r}') = 0$ outside the anomaly and 1 inside.

The problem is to infer the volume and shape of the anomaly via $\theta(\vec{r}')$ from the scattered far-field displacement u^s :

$$u^s(\vec{k}) = S e^{-ik_o r}/r, \\ S = \frac{k_o^2}{4\pi\rho\omega^2} \int d\vec{r} e^{+i\vec{k} \cdot \vec{r}} \vec{v}(\vec{r})u(\vec{r}) . \tag{9}$$

This simplified synthetic problem includes all the essential ingredients of the coupled wave problem formulated in tensor notation.

For the ME analysis we discretized the 2D region into square cells Δ on a side, identified by subscripts, and write (6) as

$$u(\vec{r}_i) = u^0(\vec{r}_i) + \sum_k \frac{e^{-i\vec{k}_o \cdot \vec{R}}}{k R(\vec{r}_i, \vec{r}_k)} u(\vec{r}_k) \tilde{\theta}(\vec{r}_k) \tag{10}$$

(with special evaluation for the $k=i$ term),

$$\text{with } \tilde{\theta}(\vec{r}_k) = \frac{k_o^2}{4\pi} \frac{\delta\rho}{\rho} \theta(\vec{r}_k), \quad \Delta A/\ell^2 = 1 . \tag{11}$$

The scattered field in the direction $\vec{k}_i = \hat{r}_i k_o$ is

$$u^s(\vec{k}_i) = \sum_n e^{-i\vec{k}_i \cdot \vec{r}_k} u(\vec{r}_k) \tilde{\theta}(\vec{r}_k) . \tag{12}$$

ME Resolution of $\tilde{\theta}$ by a "Raypath" Approach

In this ME method, promising for tomographic and geotomographic inversion, ⁵ the real (or imaginary) part of the scattered field u^s in (12) is used to resolve $\tilde{\theta}$ by interpreting the left side of (12) as the "ray" transmitted along the i^{th} path and passing through a number of cells k , where

$$D_{ik} = \text{Real} \left[e^{-i\vec{k}_i \cdot \vec{r}_k} u(\vec{r}_k) \right] \quad (\text{or Imag}) \tag{13}$$

represents the i^{th} path length in cell k . The solution is based on nonlinear ME equations for the $\tilde{\theta}_k$ in terms of Lagrange multipliers, one for each constraint (12) and one for the conservation of total $\Sigma \tilde{\theta}_k$ (unknown!). These equations were obtained by writing a function F analogous to (5) as a sum of the entropy and the constraint equations, each multiplied by a distinctive Lagrange multiplier. F was then made an extremum with respect to variations of all the $\tilde{\theta}_k$.

In principle the $\tilde{\theta}_k$ could be treated as binary quantities, and the entropy written as the number of distinct combinations of K "anomaly" cells and $N-K$ "background" cells, N being the total number of cells. The entropy would be maximized relative to K subject to satisfaction of all the constraints. For large problems, i.e., large N , this approach would require trial-and-error investigation of an enormous number of possibilities and is not practical.

Therefore we treat $\tilde{\theta}_k$ as a continuous variable and let its relative magnitude indicate the region occupied by an anomaly. The entropy is written as the logarithm of the number of distinct combinations of the $\tilde{\theta}_k$, each built up of a number n_k of building blocks $\Delta \tilde{\theta}$ (which approaches zero in the limit). The result for entropy H is

$$H = \sum_k \tilde{\theta}_k (\ln \tilde{\theta}_k - 1) \tag{14}$$

When we write objective function F as a sum of H and all the constraint equations, each consisting of the real or imaginary part of (12) for some i and multiplied by its Lagrange multiplier, and set $\partial F / \partial \tilde{\theta}_k = 0$ for all k , we obtain the ME equations for the $\tilde{\theta}_k$.

The solution is obtained by iteration: an initial guess of the β_i yields estimates $\tilde{\theta}_k$ from the ME equations, and these determine \hat{u}_i^s in (12); then the β_i are changed to bring the \hat{u}_i^s closer to the true values, and these yield updated values of $\hat{\theta}_k$; and so on. Each new solution for the $\hat{\theta}_k$ required solving (10) for the u_i in order to update the raypath D_{ik} of (13) before obtaining \hat{u}_i^s from (12).

Synthetic data examples have indicated that this method requires a more subtle algorithm for convergence than was first believed. There are two reasons for this: only half the scattered field information (Real or Imag) is utilized and the raypath D_{ik} are continually changing in the iterative procedure. Therefore we decided to abandon for the time being the investigation of this ME method.

ME Resolution of $\tilde{\theta}$ from the "Radiating Source" Viewpoint

Our equations for the analysis are again (10)-(12), but now we retain all the information in the complex radiation field u^S and solve iteratively for the radiating source distribution

$$a_k = A_k e^{i\psi_k} = u(\bar{r}_k) \tilde{\theta}(\bar{r}_k)$$

as a continuous parameter defined at the center of each cell. Factor $\exp[-ik_i \cdot \bar{r}_k]$ in (12) is the known transmission factor from cell k in the direction of \bar{k}_i .

The entropy H is defined in terms of the amplitude A_k above, with no regard for phase* ψ_k . It proved to be simpler algorithmically to define H relative to the A_k^2 rather than the A_k , so that, analogous to (14) we have

$$H = \sum_k A_k^2 (2 \ln A_k - 1) \quad (15)$$

Upon writing the objective function F as a sum of H and the complex constraint equation (12)--for a prescribed u^0 --each multiplied by a complex Lagrange multiplier β_i , and making F an extremum relative to independent variations of the real $a_{kR} = A_k \cos \psi_k$ and imaginary a_{kI} we obtained the ME equations for the a_{kR} , a_{kI} .

These equations are

$$a_{kR} = (1/2L_k) \sum_j (\beta_{jR} C_{kj} + \beta_{jI} S_{kj}) \quad (16)$$

$$a_{kI} = (1/2L_k) \sum_j (-\beta_{jR} S_{kj} + \beta_{jI} C_{kj}) \quad (17)$$

where

$$L_k \ln [(a_{kR}^2 + a_{kI}^2)/A_T], \quad A_T = \sum_k (a_{kR}^2 + a_{kI}^2) \quad (18)$$

*It appears now that this method does not predict source phases as accurately as formerly believed.

$$C_{kj} = \cos \theta_{kj}, \quad \theta_{kj} = \frac{\omega r_k}{c} \cos (\theta_k - \theta_j) \tag{19}$$

$$S_{kj} = \sin \theta_{kj} \tag{20}$$

Manipulation of (16) and (17) and use of the constraint Eq. (12) yields well determined equations for the β_{jR} , β_{jI} which are solved each iteration,

$$\sum_j (f_{j'j} \beta_{jR} + G_{j'j} \beta_{jI} = u_j^s{}_R \tag{21}$$

$$\sum_j (-G_{j'j} \beta_{jR} + F_{j'j} \beta_{jI}) = u_j^s{}_I \tag{22}$$

in which

$$f_{j'j} = 1/2 \sum_k (C_{kj} C_{kj'} + S_{kj} S_{kj'}) / L_k \tag{23}$$

$$G_{j'j} = 1/2 \sum_k (S_{kj} C_{kj'} - C_{kj} S_{kj'}) / L_k \tag{24}$$

The algorithm iterates to a solution of (16)-(24) as follows: after solving initially all the L_k assumed equal, the β_{jR} , β_{jI} are solved by (21) and (22). A_T was set just large enough to enable solution for each a_{kR} , a_{kI} by (16) and (17). a_{kI} was obtained as a multiple of a_{kR} by dividing (17) by (16) and a_{kR} was obtained by trial and error solution of (16), with A_T fixed in L_k . After obtaining all the a_{kR} , a_{kI} , A_T was updated, then the new L_k found. The new $F_{j'j}$ and $G_{j'j}$ were obtained from (23) and (24). The algorithm then returned to the starting point and resolved all the β_j by (21) and (22) and continued on until satisfactory convergence was reached.

The algorithm converged well enough to enable clear resolution of synthetic data examples such as described in the next section. We verified the accuracy of each solution by checking that the entropy was essentially maximum relative to changes in the a_{kR} , a_{kI} . However, we have not been able to prove that there is only one maximum and not two or more local maxima.

An Example of the "Radiating Source" ME Method

We now offer a rather impressive example of the application of (12) to obtain the $u_k \tilde{\theta}_k$ -distribution consistent with (10). Figure 2 shows a background region of 100 cells, containing the irregularly shaped 10-cell anomaly. The side of the region probed was assumed to be 2 wavelengths at the operating frequency, which made each cell .2λ square.

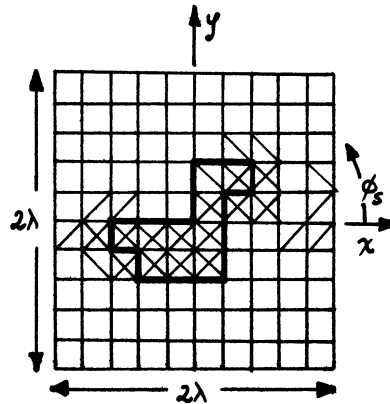


Fig. 2. Two dimensional anomaly and its resolution by the "radiating source" ME method.

We assumed the $\tilde{\theta}$ parameter of (11) had the value -1 fixed by $k_0 = 2\pi/\lambda$ and $\delta\rho/\rho$. A different frequency would, of course, change $\tilde{\theta}$. We solved (10) for u_i and generated the appropriate "measured" scattered field u^s in various directions \bar{k}_i according to (12).

For an incident plane wave u^0 propagating in the $-x$ direction at $\phi_s = 0$ we fed into the ME inversion algorithm scatter data u^s in 20 directions, equally spaced in angle from $+90^\circ$ to -81° . In solving (21), (22) for the β each iteration by LU decomposition and back substitution some of the pivot elements were miniscule ($\approx 10^{-10}$) but eigenvector decomposition was not necessary and the algorithm converged on a solution in about ten iterations.

For u^0 incident along the $-x$ direction the 20 cells of largest magnitude $u_k \tilde{\theta}_k$ are indicated by the lines slanting upward and to the right in Fig. 2. All the cells of the actual anomaly are included in this ME group of largest magnitude. Eight of the ten anomaly cells are included among the first nine cells of largest $|u_k \tilde{\theta}_k|$. The magnitude of this quantity ranged from 0.75 to 0.29 in the ME group of 20 cells because the magnitude of u was considerably less than 1.

We then repeated the analysis for a wave u^0 incident from the $\phi_s = 30^\circ$ direction. The ME group of 20 cells of largest magnitude are identified by the lines slanting upward and to the left. The magnitudes ranged from .102 to .025.

All but one of the anomalous-region cells are included in both groups of 20 cells each. Five cells outside the anomaly are also included in both these ME groups. One can reasonably conclude from this work that an anomaly does exist, and its leftmost boundary is ambiguous by two cells and its rightmost boundary is ambiguous by three cells!

We emphasize that this example was not selected as the best one of a group; in fact it is the first non-trivial example we chose for investigating the potential of this ME method for NDE resolution of anomalies in materials.

ULTRASONIC FLAW CHARACTERIZATION BY THE BOUNDARY INTEGRAL EQUATION METHOD⁷

Instead of characterizing the scattering by a volume integral equation of the Fredholm type (6), we could employ a surface integral equation. If we discretized the region of interest into cells we could, in principle, treat each cell edge in two dimensions (or cell face in three dimensions) as a binary quantity: either on the anomaly or not on it. However, this would require investigation of an impractical number of sizes and shapes even for moderate problems. The alternative is to treat the scattering from every edge or face as a continuous quantity and find the most likely boundary subject to the data.

In two dimensions we would have to resolve approximately $2N^2$ scattering edges in an $N \times N$ region, compared to N^2 scattering areas by the volume integral Fredholm equation. In three dimensions we would have nearly three times more faces to resolve than cell volumes. Therefore, these elementary considerations indicate no advantage in taking a maximum entropy viewpoint of anomaly characterization by a boundary integral equation method.

CONCLUSIONS ABOUT THE ME "RADIATING SOURCE" METHOD OF INVERSION

Although we have concentrated on only one simplified, synthetic-data example of NDE inversion, and a two dimensional one at that, we can infer some tentative conclusions from it and related ME work.^{5,6}

Clearly we should have enough scatter data to resolve all of the anomaly reasonably well; without knowledge of its shape one should increase the number of processed data and study the convergence to a (fuzzy) shape. Yet the number of data should not be comparable to the number of unknowns (cells) because the algorithm would become very ill conditioned. We suggested the following inequality be satisfied in practice:

$$N_A < J_S \lesssim K/2,$$

with N_A = number of anomaly cells inferred, J_S = number of scatter data (complex) for reasonable resolution of N_A , and K , the number of cells in the region under study.

The overall size in wavelengths of the region probed is not crucial provided each cell size is comparable to the wavelength.

Scatter data need not be taken in all directions to resolve an anomaly; data reflected into the half-space for several incident waves should suffice.

The method does not inherently favor single-volume scatterers; disjoint anomalies might be well resolved.

This particular ME method is expected to be more successful if the constraints limit more tightly the number of possible solutions. This is fortunate from a practical standpoint, for it implies that, when an incident wave (compressional or shear) generates both compressional and shear scattered waves of more than one coordinate component each, the additional scatter data will resolve the anomaly even more sharply. Note that the ME method does not depend on iterating solutions of the Fredholm integral equation which describes the displacements.

Regarding noise in the data, synthetic data examples of seismic parameter inversion by an ME "raypath" approach⁵ indicate that, as the noise increases, the resolution of strong anomalies is not at first severely impaired. We have, as yet, made no studies of the effect of noise in the ME "radiating source" method.

Finally, we observe that the evaluation of any ME method of inversion is a subjective one, and the ME "radiating source" method has at least one variation. It could be based on entropy formulated in terms of amplitude of cell parameter rather than amplitude squared--as was done above. But regardless of how it is formulated, the ME technique may be employed with reasonable effort for two purposes: (1) to obtain a "most probable" solution to an inversion problem with a minimum number of assumptions, and (2) to assess the reasonableness of an inversion by another method.

REFERENCES

1. B.T. Khuri-Yakub C.H. Chow, K. Liang and G.S. Kino, "NDE for Bulk Defects in Ceramics," Proceedings of the DARPA/AFWAL Review of Progress in Quantitative NDE, AFWL-TR-81,4080, Rockwell International Science Center, January 1981.
2. B.H. Soffer and R. Kikuchi, "Maximum Entropy Image Estimation, Analysis of Image Formation with Thinned Random Arrays," Hughes Research Laboratory, Malibu, CA, 1981.

3. S.J. Wernecke and L.R. D'Addario, "Maximum Entropy Image Reconstruction," IEEE Trans. Comp., 26:351, 1977.
4. J.E. Gubernatis, "Elastic Wave Scattering Calculations and the Matrix Variational Pade Approximation Method," Proceedings of the DARPA/AFWAL Review of Progress in Quantitative NDE, AFWL-TR-81-4080, Rockwell International Science Center, January 1981.
5. R.M. Bevensee, "Solution of Underdetermined Electromagnetic and Seismic Problems by the Maximum Entropy Method," IEEE Trans. Ant. Prop., 29:271, 1981,
6. R.M. Bevensee, "Maximum Entropy Resolution of Two Dimensional Antenna Distributions," in Antennas and Propagation, Part 1, IEEE Conference Publication No. 195, 1981.
7. L.W. Schmerr, Jr. and C. Sieck, "Ultrasonic Flaw Characterization in the Resonance Regime by the Boundary Integral Equation Method," Proceedings of the DARPA/AFWAL Review of Progress in Quantitative NDE, AFWL-TR-81, 4080, Rockwell International Science Center, January 1981.

ACKNOWLEDGEMENT

This work was performed under the auspices of the U.S. Department of Energy by Lawrence Livermore National Laboratory under Contract No. W-7405-Eng-48.